Imaginex International Journal of Interdisciplinary Research and Reviews (IIJIRR)
Volume 1, Issue 3, November – December 2026
ISSN: 3140-0094 (Online)
www.iijirr.com

Closed-Form Degree-Based Topological Indices of Body-Centred Cubic Strut-Lattice Graphs for Additively Manufactured Cellular Structures

M. K. Vediappan[1], K. Srinivasan[1,*]

[1]Department of Mathematics, Vels Institute of Science, Technology and Advanced Studies (VISTAS), Pallavaram, Chennai 600117, Tamil Nadu, India

[*]Corresponding author: K. Srinivasan (e-mail: srisaius@gmail.com)

Abstract

Strut-based lattice structures produced by additive manufacturing are naturally described as graphs, in which nodes are strut junctions and edges are struts. This paper derives exact edge partitions, by end-vertex degrees, for three lattice graph families used in practice: the body-centred cubic lattice (BCC), the body-centred cubic lattice with vertical struts (BCCz) and the simple cubic lattice (SC), each built from $n \times n \times n$ unit cells. From these partitions it obtains closed forms for eight vertex-degree-based topological indices of the BCC lattice and for the Zagreb, forgotten and harmonic indices of the BCCz and SC lattices. For the BCC lattice, a product structure in the vertex degrees is identified that collapses several indices into compact cubes; for example, the second Zagreb index equals $64(2n-1)^3$ and the Randić index equals $(n-1+\sqrt{2})^3$. All formulas were checked against direct computation on explicitly generated graphs for every n up to 10, with zero discrepancy. Normalising the indices by edge count shows that boundary nodes dominate the indices at the specimen sizes used in mechanical testing: at $n = 5$, about 70% of the lattice-point nodes of the BCC graph lie on the boundary, and the per-edge Randić index remains 13% above its bulk limit even at $n = 10$. The average nodal degree tends to 8, 9 and 6 for BCC, BCCz and SC respectively. All three values are below the connectivity of 12 that a periodic lattice with similarly situated nodes needs to be stretching-dominated, so the BCC lattice is expected to deform mainly by strut bending, although the struts of the SC lattice and the vertical struts of the BCCz lattice can still carry loads along their own axes by stretching. The results provide exact, size-dependent graph descriptors for lattice design that can be tested in future structure–property studies of additively manufactured cellular materials.

Keywords: Topological index, Zagreb index, Randić index, atom-bond connectivity index, lattice structure, body-centred cubic lattice, additive manufacturing

1. Introduction

Additive manufacturing, and selective laser melting in particular, has made it practical to build strut-based lattice structures whose mechanical, thermal and acoustic behaviour can be tuned through the choice of unit cell and strut geometry [1]. Among the many unit cells in use, the body-centred cubic (BCC) cell and its variant with additional vertical struts (BCCz) are widely studied, and the simple cubic (SC) cell is a common reference geometry [1]. The way struts are connected at the nodes governs whether a lattice deforms mainly by strut bending or by strut stretching. Maxwell's rule gives a necessary condition for a pin-jointed frame to be rigid; for a large three-dimensional frame it requires an average nodal connectivity of at least 6 [2]. Deshpande, Ashby and Fleck showed that nodal connectivity is the controlling topological quantity, and that a periodic lattice whose nodes are all similarly situated needs a connectivity of 12 to be rigid and stretching-dominated [3].

A lattice is, at the level of its connectivity, a graph. Chemical graph theory has developed a large family of graph invariants, known as topological indices, that condense the degree structure of a graph into single numbers. The first and second Zagreb indices were introduced by Gutman and Trinajstić [4], the connectivity (Randić) index by Randić [5], the atom-bond connectivity (ABC) index by Estrada et al. [6], the geometric–arithmetic (GA) index by Vukičević and Furtula [7], the sum-connectivity index by Zhou and Trinajstić [8], the harmonic index by Fajtlowicz [9], and the forgotten (F) index was re-examined by Furtula and Gutman [10]. A critical review of the degree-based indices is given by Gutman [11]. These indices have been computed for many molecular graphs and interconnection networks, and for some crystal-lattice graphs: degree-based indices of the face-centred cubic lattice have been derived [12], and the Wiener and Kirchhoff indices of body-centred cubic grids have been studied [13], [14]. The simple cubic lattice is a Cartesian product of three paths, so its Zagreb indices also follow from general product formulas [15]. In lattice mechanics, truss lattices are now often represented as graphs for design and property prediction [16]–[18]. To the best of our knowledge, however, closed-form degree-based indices of the finite BCC and BCCz strut-lattice graphs used for additively manufactured specimens have not been reported.

This paper addresses that gap for three lattice families. The specific contributions are:

- complete edge partitions, by end-vertex degrees, of the BCC, BCCz and SC lattice graphs of n × n × n unit cells;
- exact closed forms for eight degree-based indices of the BCC lattice, including a product lemma that reduces the second Zagreb, Randić and related indices to perfect cubes;
- closed forms for the Zagreb, forgotten and harmonic indices of the BCCz and SC lattices (for SC, the Zagreb indices also follow from general Cartesian-product formulas [15] and are included for comparison);
- per-edge limits and average-degree limits that separate boundary effects from bulk behaviour, with every result checked against direct computation on explicitly generated graphs.

2. Preliminaries

2.1. Degree-based topological indices

Let G = (V, E) be a simple connected graph and let d_u denote the degree of vertex u. The indices studied here are sums over edges of a function of the two end-vertex degrees:

$$M_1(G) = \sum_{uv\in E} (d_u + d_v), \qquad M_2(G) = \sum_{uv\in E} d_u d_v \tag{1}$$

$$F(G) = \sum_{uv\in E} (d_u^2 + d_v^2), \qquad R(G) = \sum_{uv\in E} \frac{1}{\sqrt{d_u d_v}} \tag{2}$$

$$SCI(G) = \sum_{uv\in E} \frac{1}{\sqrt{d_u + d_v}}, \qquad H(G) = \sum_{uv\in E} \frac{2}{d_u + d_v} \tag{3}$$

$$GA(G) = \sum_{uv\in E} \frac{2\sqrt{d_u d_v}}{d_u + d_v}, \qquad ABC(G) = \sum_{uv\in E} \sqrt{\frac{d_u + d_v - 2}{d_u d_v}} \tag{4}$$

If $m_{ij}(G)$ denotes the number of edges whose end vertices have degrees i and j (i ≤ j), every index of this type with edge function f can be written as

$$TI(G) = \sum_{i\le j} m_{ij}(G)\, f(i, j) \tag{5}$$

so that the whole problem reduces to finding the edge partition $\{m_{ij}\}$.

2.2. Lattice graph models

For a positive integer n, the lattice points are the integer triples (i, j, k) with 0 ≤ i, j, k ≤ n, and the unit cells are the cubes [i, i+1] × [j, j+1] × [k, k+1] with 0 ≤ i, j, k ≤ n − 1. Three graphs are defined on these points (Figure 1).

- **BCC(n)**: one body-centre vertex is placed in each cell and joined to the eight corners of that cell. Hence $|V| = (n + 1)^3 + n^3 = (2n + 1)(n^2 + n + 1)$ and $|E| = 8n^3$.
- **BCCz(n)**: BCC(n) together with the vertical struts joining (i, j, k) to (i, j, k + 1). This adds $n(n + 1)^2$ edges, so $|E| = n(9n^2 + 2n + 1)$.
- **SC(n)**: the lattice points joined by unit struts parallel to the three axes, i.e. the Cartesian product $P_{n+1} \square P_{n+1} \square P_{n+1}$ of paths, with $|V| = (n + 1)^3$ and $|E| = 3n(n + 1)^2$.

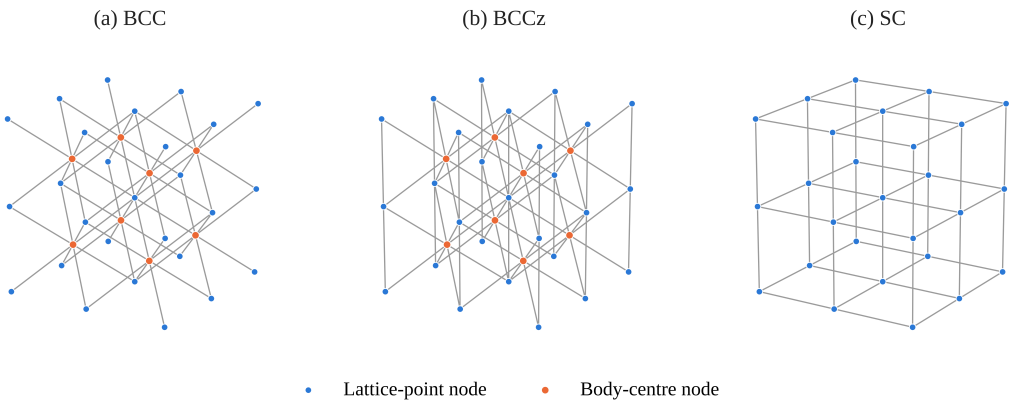

Figure 1. The three lattice graphs for n = 2: (a) BCC, (b) BCCz and (c) SC. Lattice-point vertices are shown in blue and body-centre vertices in orange.

3. Main results

3.1. The BCC lattice

For a coordinate $x \in \{0, 1, \ldots, n\}$ define $a(x) = 1$ if $x \in \{0, n\}$ and $a(x) = 2$ otherwise; $a(x)$ is the number of unit intervals of $[0, n]$ that contain x.

Lemma 1. *In BCC(n), every body-centre vertex has degree 8, and the lattice point $v = (i, j, k)$ has degree $c(v) = a(i)a(j)a(k)$. Consequently the edge partition of BCC(n), $n \geq 1$, is $m_{1,8} = 8$, $m_{2,8} = 24(n - 1)$, $m_{4,8} = 24(n - 1)^2$ and $m_{8,8} = 8(n - 1)^3$.*

Proof. A body-centre vertex is joined only to the eight corners of its cell. A lattice point is joined to the centre of every cell containing it, and the cells containing (i, j, k) are the products of the $a(i)$, $a(j)$ and $a(k)$ admissible unit intervals in each coordinate. If t coordinates of v lie strictly between 0 and n, then $c(v) = 2^t$; there are 8, $12(n - 1)$, $6(n - 1)^2$ and $(n - 1)^3$ lattice points with $t = 0, 1, 2, 3$ respectively. Every edge joins one lattice point to one centre, and a lattice point of degree 2^t carries 2^t edges, each of type $(2^t, 8)$. Multiplying the counts by 2^t gives the stated partition; the four classes sum to $8n^3 = |E|$. ∎

Because $c(v)$ factorises over the three coordinates, sums of powers of $c(v)$ factorise as well. This gives a short route to several indices.

Lemma 2 (product lemma). *For any real γ, $\Sigma_v c(v)^\gamma = (2 + (n - 1)2^\gamma)^3$, the sum running over all lattice points of BCC(n).*

Proof. By Lemma 1, $\Sigma_v c(v)^\gamma = \Sigma_{i,j,k} a(i)^\gamma a(j)^\gamma a(k)^\gamma = (\Sigma_{x=0}^{n} a(x)^\gamma)^3$, and $\Sigma_x a(x)^\gamma = 2 \cdot 1 + (n - 1)2^\gamma$. ∎

Since each lattice point v contributes $c(v)$ edges of type $(c(v), 8)$, equation (5) becomes $TI(BCC(n)) = \Sigma_v c(v) f(c(v), 8)$. Whenever $c \cdot f(c, 8)$ is a combination of powers of c, Lemma 2 evaluates the sum at once.

Theorem 1. *For $n \geq 1$ and $m = n - 1$, the BCC lattice graph satisfies*

$$M_1 = 8(2n-1)^3 + 64n^3, \qquad M_2 = 64(2n-1)^3, \qquad F = 8(4n-3)^3 + 512n^3 \tag{6}$$

$$R = \left(n - 1 + \sqrt{2}\right)^3 \tag{7}$$

$$SCI = 2m^3 + 4\sqrt{3}\,m^2 + \frac{12\sqrt{10}}{5}\,m + \frac{8}{3} \tag{8}$$

$$H = m^3 + 4m^2 + \frac{24}{5}\,m + \frac{16}{9} \tag{9}$$

$$GA = 8m^3 + 16\sqrt{2}\,m^2 + \frac{96}{5}\,m + \frac{32\sqrt{2}}{9} \tag{10}$$

$$ABC = \sqrt{14}\,m^3 + 6\sqrt{5}\,m^2 + 12\sqrt{2}\,m + 2\sqrt{14} \tag{11}$$

Proof. For M_2, $c \cdot (8c) = 8c^2$ and Lemma 2 with $\gamma = 2$ gives $8(2 + 4m)^3 = 64(2n - 1)^3$. For M_1, $c(c + 8) = c^2 + 8c$ gives $(2 + 4m)^3 + 8(2 + 2m)^3 = 8(2n - 1)^3 + 64n^3$. For F, $c(c^2 + 64) = c^3 + 64c$ gives $(2 + 8m)^3 + 64(2 + 2m)^3 = 8(4n - 3)^3 + 512n^3$. For R, $c/\sqrt{(8c)} = c^{1/2}/(2\sqrt{2})$ and Lemma 2 with $\gamma = 1/2$ gives $(2 + \sqrt{2}\,m)^3/(2\sqrt{2}) = (m + \sqrt{2})^3$. The remaining four indices follow from equation (5) and Lemma 1; for example, $H = 8 \cdot (2/9) + 24m \cdot (2/10) + 24m^2 \cdot (2/12) + 8m^3 \cdot (2/16)$, which simplifies to equation (9). Equations (8), (10) and (11) are obtained in the same way. ∎

For $n = 1$ the graph BCC(1) is the star $K_{1,8}$, and equations (6)–(11) reduce to the known star values, for example $M_2(K_{1,8}) = 64$ and $R(K_{1,8}) = 2\sqrt{2}$.

3.2. The BCCz lattice

Adding vertical struts raises the degree of a lattice point (i, j, k) by one if $k \in \{0, n\}$ and by two otherwise, while the body-centre vertices keep degree 8. Classifying lattice points by which of their coordinates lie on the boundary and by the type of each incident strut gives the partition in Table 1.

Table 1. Edge partition of BCCz(n) for $n \geq 2$.

(d_u, d_v)	Number of edges	(d_u, d_v)	Number of edges
(2, 4)	8	(5, 8)	$8(n - 1)^2$
(2, 8)	8	(5, 10)	$2(n - 1)^2$
(3, 6)	$8(n - 1)$	(6, 6)	$4(n - 1)(n - 2)$
(3, 8)	$16(n - 1)$	(6, 8)	$16(n - 1)^2$
(4, 4)	$4(n - 2)$	(8, 10)	$8(n - 1)^3$
(4, 8)	$8(n - 1)$	(10, 10)	$(n - 1)^2(n - 2)$

Theorem 2. *For n ≥ 2, the BCCz lattice graph satisfies*

$$M_1 = 164n^3 - 106n^2 + 48n - 10, \qquad M_2 = 740n^3 - 988n^2 + 460n - 84 \tag{12}$$

$$F = 1512n^3 - 1886n^2 + 1244n - 294 \tag{13}$$

$$H = \frac{89}{90}n^3 + \frac{1888}{1365}n^2 + \frac{55907}{90090}n + \frac{823}{3003} \tag{14}$$

Proof. Substitute the partition of Table 1 into equations (1)–(3) and (5) and collect powers of n. ∎

The R, SCI, GA and ABC indices of BCCz(n) follow from Table 1 and equation (5) in the same way; their numerical values are listed in Table 3.

3.3. The SC lattice

Lemma 3. *For n ≥ 2 the edge partition of SC(n) is $m_{3,4} = 24$, $m_{4,4} = 12(n - 2)$, $m_{4,5} = 24(n - 1)$, $m_{5,5} = 12(n - 1)(n - 2)$, $m_{5,6} = 6(n - 1)^2$ and $m_{6,6} = 3(n - 1)^2(n - 2)$.*

Proof. A lattice point with t interior coordinates has degree 3 + t. Edges of each type are counted along the 12 cube edges (degrees 3 and 4), on the 6 faces (degrees 4 and 5) and in the interior (degrees 5 and 6); the six classes sum to $3n(n + 1)^2$. ∎

Theorem 3. *For n ≥ 2, the SC lattice graph satisfies*

$$M_1 = 36n^3 + 42n^2 - 6, \qquad M_2 = 108n^3 + 48n^2 - 48n - 12 \tag{15}$$

$$F = 216n^3 + 102n^2 - 84n - 18, \qquad H = \frac{n^3}{2} + \frac{82}{55}n^2 + \frac{479}{330}n + \frac{479}{1155} \tag{16}$$

Proof. Substitute Lemma 3 into equations (1)–(3) and (5). As a check, the Zagreb indices in equation (15) agree with the Cartesian-product formulas of [15] applied to $P_{n+1} \square P_{n+1} \square P_{n+1}$. ∎

3.4. Bulk limits

Corollary 1. *As $n \to \infty$, the per-edge indices $R/|E|$, $GA/|E|$ and $ABC/|E|$ converge to 1/8, 1 and $\sqrt{14}/8 \approx 0.468$ for BCC; to 1/6, 1 and $\sqrt{10}/6 \approx 0.527$ for SC; and to $(2/\sqrt{5} + 1/10)/9 \approx 0.110$, $(32\sqrt{5}/9 + 1)/9 \approx 0.994$ and $(8/\sqrt{5} + 3\sqrt{2}/10)/9 \approx 0.445$ for BCCz. The average degree $2|E|/|V|$ tends to 8, 9 and 6 respectively.*

Proof. In each lattice the edges between interior vertices form the only class of order n^3. In BCC these are the $8(n - 1)^3$ edges of type (8, 8); in SC, the $3(n - 1)^2(n - 2)$ edges of type (6, 6); in BCCz, the $8(n - 1)^3$ edges of type (8, 10) and the $(n - 1)^2(n - 2)$ edges of type (10, 10), in the ratio 8 : 1. Dividing by |E| and letting $n \to \infty$ gives the per-edge limits. The degree limits follow from |E| and |V| in Section 2.2. ∎

4. Verification and discussion

4.1. Computational verification

Each lattice graph was generated explicitly in NetworkX [19] for every n from 1 (BCC) or 2 (BCCz, SC) up to 10, and its edge partition and all eight indices were computed directly from the vertex degrees. The partitions in Lemmas 1 and 3 and Table 1 matched the direct counts exactly for every n, and the closed forms (6)–(16) reproduced the directly computed index values with zero discrepancy to machine precision. Table 2 lists the vertex and edge counts of the three graphs, and selected index values are listed in Table 3.

Table 2. Size of the three lattice graphs.

Lattice	|V|	|E|	Limit of 2|E|/|V|
BCC	$(2n + 1)(n^2 + n + 1)$	$8n^3$	8
BCCz	$(2n + 1)(n^2 + n + 1)$	$n(9n^2 + 2n + 1)$	9
SC	$(n + 1)^3$	$3n(n + 1)^2$	6

4.2. Boundary effects at practical specimen sizes

Lattice specimens built for compression testing typically contain only a few unit cells per side. At such sizes a large share of the vertices lie on the boundary and have reduced degree. For BCC(n) the fraction of lattice points on the boundary is $1 - (n - 1)^3/(n + 1)^3$, which equals 70.4% at n = 5 and is still 25.9% at n = 20. Figure 2 shows the consequence for the per-edge indices: they approach their bulk limits only slowly, at rate O(1/n). By equation (7), $R/|E|$ for BCC equals $(n - 1 + \sqrt{2})^3/(8n^3)$, which is still 13% above its limit of 1/8 at n = 10. Index values measured on, or computed for, small specimens therefore describe a boundary-dominated graph rather than the bulk lattice, and comparisons between lattices should be made at equal n.

Table 3. Index values for n = 2, 5 and 10.

Lattice	n	M_1	M_2	R	SCI	H	GA	ABC	F
BCC	2	728	1,728	14.07	19.18	11.58	54.86	41.61	5,096
	5	13,832	46,656	158.71	271.88	148.98	955.87	529.49	103,304
	10	118,872	438,976	1,129.48	2,090.16	1,097.98	7,842.65	3,974.62	917,224
BCCz	2	974	2,804	16.15	24.49	14.96	76.74	47.37	6,746
	5	18,080	70,016	165.85	306.69	161.57	1,156.21	581.77	147,776
	10	153,870	645,716	1,149.19	2,275.88	1,133.68	9,107.81	4,309.52	1,335,546
SC	2	450	948	13.39	18.88	13.28	53.58	32.98	1,950
	5	5,544	14,448	107.72	169.85	107.45	538.76	304.27	29,112
	10	40,194	112,308	664.76	1,095.95	664.02	3,626.40	1,981.59	225,342

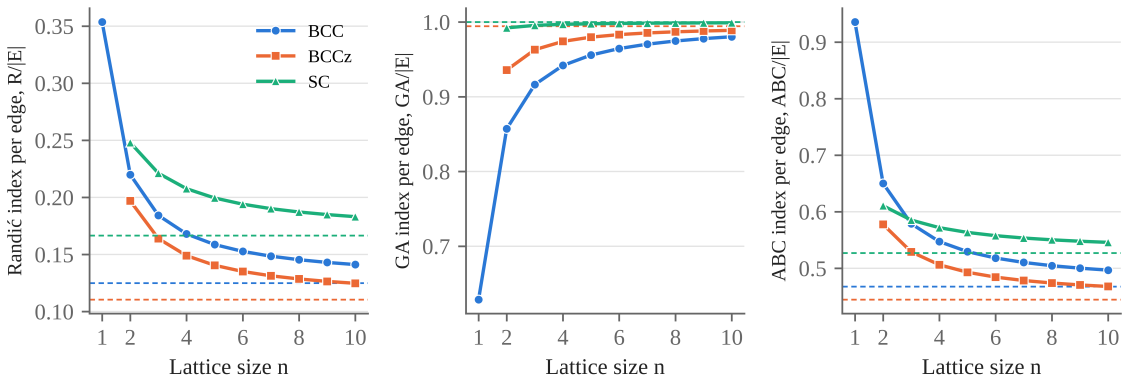

Figure 2. Per-edge Randić, GA and ABC indices against lattice size n. Dashed lines mark the bulk limits of Corollary 1.

The three lattices are ordered differently by different indices. For n ≥ 3 the per-edge Randić and ABC indices rank SC above BCC above BCCz, mirroring their average degrees in reverse, because both indices decrease as end-vertex degrees grow. The GA index, which depends only on the ratio of the two end-vertex degrees, is close to 1 for all three lattices once interior edges dominate. It is therefore a measure of degree heterogeneity rather than of connectivity, and it separates the lattices mainly at small n, where BCC has the most heterogeneous edges.

4.3. Connectivity and deformation mode

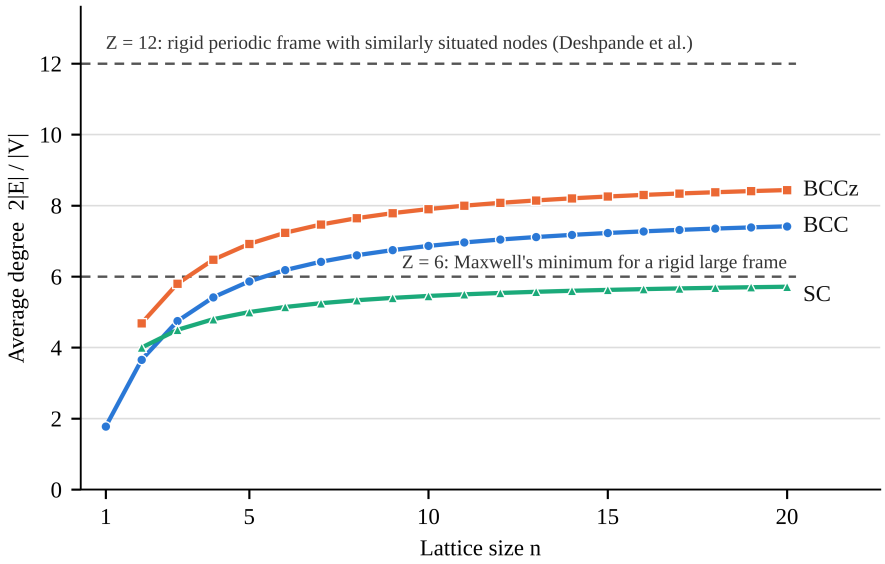

Figure 3. Average degree of the three lattice graphs against lattice size n. Dashed lines mark Maxwell's minimum average connectivity for rigidity of a large three-dimensional frame (6) [2] and the connectivity of 12 needed for rigidity of a periodic frame with similarly situated nodes [3].

Figure 3 shows the average degree 2|E|/|V| for n up to 20: the BCC lattice approaches 8, BCCz approaches 9 and SC approaches 6. Maxwell's rule requires an average connectivity of at least 6 for a large three-dimensional pin-jointed frame to be rigid [2], but this condition is necessary rather than sufficient. A periodic lattice whose nodes are all similarly situated needs a connectivity of 12 to be rigid and stretching-dominated [3]. In the bulk of the BCC lattice all nodes are similarly situated, each with 8 struts, so the BCC lattice is expected to deform predominantly by strut bending. The SC lattice meets only Maxwell's minimum of 6; it resists shear by strut bending, although its struts carry loads along their own axes by stretching. The BCCz lattice has two kinds of node (10 struts at interior lattice points and 8 at body centres), so the criterion of [3] does not apply to it directly, and its vertical struts carry vertical loads by stretching. The average degree is therefore a useful but incomplete guide to the deformation mode. Adding vertical struts (BCCz) raises the average degree by one in the limit, and the corresponding increase in the Zagreb indices (compare equations (6) and (12)) gives a direct, size-resolved measure of the added connectivity.

Degree-based indices capture only the topology of a lattice. They do not include strut length, cross-section or material, and they cannot by themselves predict stiffness or strength. Their value lies in providing exact, reproducible descriptors that can be combined with geometric parameters in structure–property models; no such correlation is tested here. Natural extensions are distance-based indices such as the Wiener index, other unit cells such as face-centred cubic and octet lattices, and correlation of the indices with measured properties of printed specimens.

5. Conclusion

Exact edge partitions and closed-form degree-based topological indices were derived for the BCC, BCCz and SC lattice graphs of n × n × n unit cells. For the BCC lattice, a product lemma reduces the second Zagreb and Randić indices to the perfect cubes $64(2n-1)^3$ and $(n-1+\sqrt{2})^3$, and gives similarly compact forms for the first Zagreb and forgotten indices. All results were confirmed by direct computation for n up to 10. The analysis shows that boundary vertices dominate the indices at typical specimen sizes. It also shows that the average degree of all three lattices stays below the connectivity of 12 needed for a rigid periodic lattice with similarly situated nodes: the BCC lattice is expected to be bending-dominated, whereas the struts of the SC lattice and the vertical struts of the BCCz lattice can still carry loads along their axes by stretching. The formulas give lattice designers exact, size-dependent topological descriptors that can be tested in future structure–property studies of additively manufactured cellular materials.

Declarations

Conflict of interest. The authors declare that they have no known competing financial interests or personal relationships that could have appeared to influence the work reported in this paper.

Funding. This research did not receive any specific grant from funding agencies in the public, commercial, or not-for-profit sectors.

Data availability. The code used to generate the lattice graphs and verify the formulas is available from the corresponding author on request.

Use of generative AI. During the preparation of this work the authors used a generative AI tool to a limited extent for language editing and proofreading. After using this tool, the authors reviewed and edited the content as needed and take full responsibility for the content of the publication.

Ethics approval and consent. Not applicable. This study is purely mathematical and involves no human participants, animals or personal data.

Author contributions. M. K. Vediappan and K. Srinivasan contributed equally to this work. Both authors read and approved the final manuscript.

References

[1] T. Maconachie, M. Leary, B. Lozanovski, X. Zhang, M. Qian, O. Faruque, and M. Brandt, "SLM lattice structures: Properties, performance, applications and challenges," *Materials & Design*, vol. 183, Art. no. 108137, 2019, doi: 10.1016/j.matdes.2019.108137.

[2] J. C. Maxwell, "On the calculation of the equilibrium and stiffness of frames," *The London, Edinburgh, and Dublin Philosophical Magazine and Journal of Science*, vol. 27, no. 182, pp. 294–299, 1864, doi: 10.1080/14786446408643668.

[3] V. S. Deshpande, M. F. Ashby, and N. A. Fleck, "Foam topology: bending versus stretching dominated architectures," *Acta Materialia*, vol. 49, no. 6, pp. 1035–1040, 2001, doi: 10.1016/S1359-6454(00)00379-7.

[4] I. Gutman and N. Trinajstić, "Graph theory and molecular orbitals. Total π-electron energy of alternant hydrocarbons," *Chemical Physics Letters*, vol. 17, no. 4, pp. 535–538, 1972, doi: 10.1016/0009-2614(72)85099-1.

[5] M. Randić, "Characterization of molecular branching," *Journal of the American Chemical Society*, vol. 97, no. 23, pp. 6609–6615, 1975, doi: 10.1021/ja00856a001.

[6] E. Estrada, L. Torres, L. Rodríguez, and I. Gutman, "An atom-bond connectivity index: Modelling the enthalpy of formation of alkanes," *Indian Journal of Chemistry*, vol. 37A, no. 10, pp. 849–855, 1998.

[7] D. Vukičević and B. Furtula, "Topological index based on the ratios of geometrical and arithmetical means of end-vertex degrees of edges," *Journal of Mathematical Chemistry*, vol. 46, no. 4, pp. 1369–1376, 2009, doi: 10.1007/s10910-009-9520-x.

[8] B. Zhou and N. Trinajstić, "On a novel connectivity index," *Journal of Mathematical Chemistry*, vol. 46, no. 4, pp. 1252–1270, 2009, doi: 10.1007/s10910-008-9515-z.

[9] S. Fajtlowicz, "On conjectures of Graffiti-II," *Congressus Numerantium*, vol. 60, pp. 187–197, 1987.

[10] B. Furtula and I. Gutman, "A forgotten topological index," *Journal of Mathematical Chemistry*, vol. 53, no. 4, pp. 1184–1190, 2015, doi: 10.1007/s10910-015-0480-z.

[11] I. Gutman, "Degree-based topological indices," *Croatica Chemica Acta*, vol. 86, no. 4, pp. 351–361, 2013, doi: 10.5562/cca2294.

[12] M. K. Siddiqui, M. Imran, and M. Saeed, "Topological properties of face-centred cubic lattice," *Hacettepe Journal of Mathematics and Statistics*, vol. 49, no. 1, pp. 195–207, 2020, doi: 10.15672/hujms.546348.

[13] H. Mujahed and B. Nagy, "Wiener index on lines of unit cells of the body-centered cubic grid," in *Mathematical Morphology and Its Applications to Signal and Image Processing (ISMM 2015)*, Lecture Notes in Computer Science, vol. 9082. Cham, Switzerland: Springer, 2015, pp. 597–606, doi: 10.1007/978-3-319-18720-4_50.

[14] W. Sajjad, X.-F. Pan, and Q. tul Ain, "Computation of resistance distance with Kirchhoff index of body centered cubic structure," *Journal of Mathematical Chemistry*, vol. 62, no. 4, pp. 902–921, 2024, doi: 10.1007/s10910-023-01573-6.

[15] M. H. Khalifeh, H. Yousefi-Azari, and A. R. Ashrafi, "The first and second Zagreb indices of some graph operations," *Discrete Applied Mathematics*, vol. 157, no. 4, pp. 804–811, 2009, doi: 10.1016/j.dam.2008.06.015.

[16] T. S. Lumpe and T. Stanković, "Exploring the property space of periodic cellular structures based on crystal networks," *Proceedings of the National Academy of Sciences of the United States of America*, vol. 118, no. 7, Art. no. e2003504118, 2021, doi: 10.1073/pnas.2003504118.

[17] P. P. Meyer, C. Bonatti, T. Tancogne-Dejean, and D. Mohr, "Graph-based metamaterials: Deep learning of structure-property relations," *Materials & Design*, vol. 223, Art. no. 111175, 2022, doi: 10.1016/j.matdes.2022.111175.

[18] L. Zheng, K. Karapiperis, S. Kumar, and D. M. Kochmann, "Unifying the design space and optimizing linear and nonlinear truss metamaterials by generative modeling," *Nature Communications*, vol. 14, Art. no. 7563, 2023, doi: 10.1038/s41467-023-42068-x.

[19] A. A. Hagberg, D. A. Schult, and P. J. Swart, "Exploring network structure, dynamics, and function using NetworkX," in *Proceedings of the 7th Python in Science Conference (SciPy 2008)*, Pasadena, CA, USA, 2008, pp. 11–15, doi: 10.25080/TCWV9851.